Gas-Phase Cytosine and Cytosine-N_1-Derivatives Have 0.1-1 Nanosecond Lifetimes Near the S_1 State Minimum

Susan Blaser, Maria A. Trachsel, Simon Lobsiger, Timo Wiedmer, Hans-Martin Frey, and Samuel Leutwyler[1]*

Department of Chemistry and Biochemistry, University of Bern, Freiestrasse 3, CH-3012 Bern, Switzerland

E-mail: leutwyler@dcb.unibe.ch

Abstract

UV radiative damage to DNA is inefficient because of the ultrafast $S_1 \rightsquigarrow S_0$ internal conversion of its nucleobases. Using picosecond pump/ionization delay measurements, we find that the $S_1(^1\pi\pi^*)$ state vibrationless lifetime of gas-phase keto-amino cytosine (Cyt) is $\tau = 730$ ps or ~ 700 times longer than measured by fs pump-probe ionization at higher vibrational excess energy E_{exc}. N_1-alkylation increases the S_1 lifetime up to $\tau = 1030$ ps for N_1-ethyl-Cyt, but decreases it to 100 ps for N_1-isopropyl-Cyt. Increasing the vibrational energy to $E_{exc} = 300 - 550$ cm^{-1} decreases the lifetimes to $20 - 30$ ps. The nonradiative dynamics of S_1 cytosine is not solely a property of the amino-pyrimidinone chromophore, but is strongly influenced by the N_1-substituent. Correlated excited-state calculations predict that the gap between the $S_2(^1n_O\pi^*)$ and $S_1(^1\pi\pi^*)$ states decreases along the series of N_1-derivatives, thereby influencing the S_1 state lifetime.

*To whom correspondence should be addressed

TOC graphic

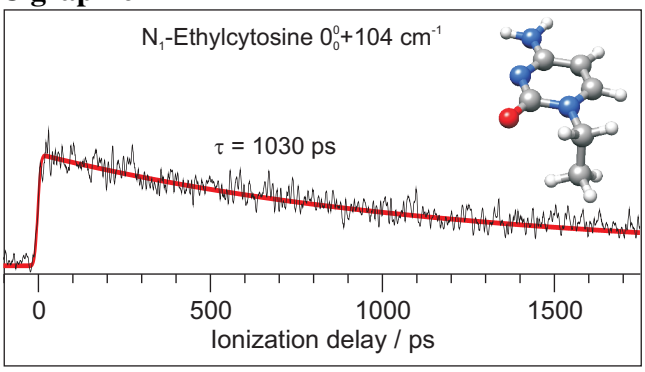

Keywords: nucleic acid bases, cytosine, picosecond dynamics,photoionization, laser spectroscopy, nonradiative processes, internal conversion

The absorption of UV light by nucleobases and the ensuing photophysical and photochemical processes constitute fundamental steps of UV-induced DNA damage, the most frequent UV photolesions involving the [2+2] photodimerization of neighboring thymine or cytosine nucleobases within a DNA strand.[1–3] In aqueous solution the canonical nucleobases, nucleosides and nucleotides exhibit S_1 state lifetimes of $\tau \sim\ 0.2 - 1.5$ ps when excited in the $260 - 270$ nm range, due to ultra-efficient $S_1 \rightsquigarrow S_0$ internal conversion.[1,2,4–10] The vibrational energy of the hot S_0 state is rapidly removed by the surrounding solvent. These properties of the nucleobase chromophores help to protect DNA and RNA from photodamage and may have allowed them to survive photolysis by the deep-UV solar radiation on prebiotic Earth, possibly leading to photochemical selection of the molecular constituents of living systems.[4,11–14]

On the surface of today's earth, however, the solar UV is cut off at $290 - 295$ nm by the ozone layer, while the long-wavelength edge of the UV absorption of cytosine (Cyt) and cytidine in aqueous solution extends to ~ 300 nm. Thus, the photobiologically and -medically relevant region of spectral overlap[1,3,11] is $290 - 300$ nm, equivalent to a range of 1150 cm^{-1}. Thus, solar UV excitation of cytosine is close to adiabatic, and very far from the Franck-Condon region. Below, we show that at S_1 vibrational excess energy $E_{exc} < 550$ cm^{-1}, gas-phase amino-keto cytosine and its N_1-derivatives exhibit lifetimes ranging from 1.03 ns to 20 picoseconds (ps), depending both

on the N_1-substituent and on the degree of vibrational excitation. While the relation between the gas-phase spectra and the red-edge of the aqueous UV absorption of Cyt is not clear, these results suggest that the solution-phase photophysics of Cyt and its derivatives might change considerably if the excitation is moved from $260 - 270$ nm to ~ 300 nm, where E_{exc} is low.

The $S_1(^1\pi\pi^*)$ state lifetimes of cytosine (Cyt) and its nucleosides and nucleotides dC, CMP and dCMP have been measured in room-temperature aqueous solution by femtosecond (fs) transient absorption and fluorescence upconversion techniques as $\tau = 0.2 - 1.2$ ps, using excitation at $263 - 270$ nm.[4,5,7–9,15] The nature of the efficient nonradiative decay mechanisms of gas phase Cyt has been investigated by calculations of its lowest electronically excited states, which predict three different conical intersections (CI) that connect the lowest $^1\pi\pi^*$ excited state to the S_0 ground state; the lowest of these is denoted the "C_5-twist" CI.[9,12,14,16–28] Spectroscopic and lifetime measurements of cold gas-phase Cyt[29–35] are crucial, because they (1) allow direct comparison to the predictions of quantum chemical calculations, (2) yield detailed insight into the excited-state structures, vibrations and nonradiative dynamics[31,32,35] and (3) can be conducted tautomer-specifically,[29–35] which is very difficult or impossible in solution. Excited-state lifetimes of jet-cooled amino-keto Cyt have been measured by femtosecond (fs) pump/delayed ionization as $\tau = 0.6 - 1.5$ ps when exciting to S_1 state vibrational energies $E_{exc} = 1500 - 4000$ cm^{-1} above the vibrationless ($v' = 0$) level.[33,34] Here we present ps pump/ionization lifetime measurements of the $v' = 0$ and lowest vibronic levels of jet-cooled keto-amino cytosine (Cyt) and its N_1-methyl, N_1-ethyl and N_1-isopropyl derivatives:

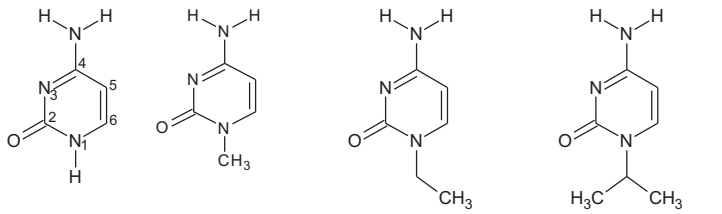

Based on a spectroscopic analysis of the Lorentzian broadening contributing to the rotational

contour widths in the 2C-R2PI spectrum of amino-keto Cyt, Lobsiger et al. determined lower lifetime limits for the S_1 $v' = 0$ level as $\tau = 45$ ps.[32] Using nanosecond (ns) pump/ionization delay measurements, the intersystem crossing (ISC) rate constants of the S_1 $v' = 0$ and low-lying levels of amino-keto Cyt have been calculated and measured.[35] The direct ps measurements in this work show that the S_1 $v' = 0$ lifetime of Cyt is ~ 15 times longer than the lower limit derived in ref. 32. The S_1 $v' = 0$ lifetime of amino-keto cytosine remains similar upon N_1-methyl substitution, increases further for the N_1-ethyl derivative, but decreases in the N_1-isopropyl-Cyt derivative.

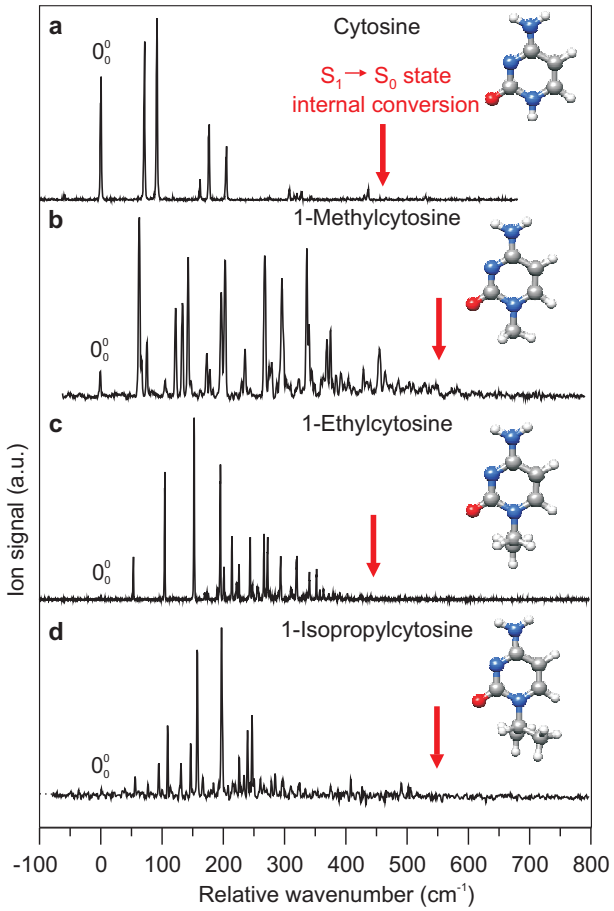

Figure 1: Nanosecond two-color resonant two-photon ionization (2C-R2PI) spectra of (a) amino-keto cytosine, (b) N_1-methyl-Cyt, (c) N_1-ethyl-Cyt, and (d) N_1-isopropyl-Cyt; ionization at 226 nm. The 0_0^0 bands are aligned at a common zero; the absolute values are (a) 31835 cm^{-1}, (b) 31852 cm^{-1}, (c) 31906 cm^{-1} and (d) 31786 cm^{-1}. Breaking-off points indicated by red arrows.

De Vries and co-workers first investigated the two-color resonant two-photon ionization (2C-R2PI)

spectra of supersonic jet-cooled Cyt, 5-methyl-Cyt and 1-methyl-Cyt, assigning the $S_0 \rightarrow S_1$ transitions of the keto-amino tautomers to bands near 32000 cm^{-1}.[29,30] The analysis of the rotational band contours later confirmed the $^1\pi\pi^*$ character of the $S_0 \rightarrow S_1$ transition of Cyt.[31,32] Fig. 1 shows the $S_0 \rightarrow S_1$ vibronic spectra of jet-cooled Cyt[29–32] and its N_1-methyl,[29] N_1-ethyl, and N_1-isopropyl derivatives, the latter two are reported for the first time. The 0_0^0 transition of N_1-methyl-Cyt was previously assigned to a band at 31916 cm^{-1}.[29] Based on UV/UV depletion and holeburning measurements we reassign it to the weaker band at 31852 cm^{-1}. Similar to Cyt, the 2C-R2PI spectra of the N_1-derivatives exhibit progressions in low-frequency out-of-plane vibrations.[31,32,36] The spectra break off at $E_{exc} \sim 450$ cm^{-1} for Cyt, ~ 550 cm^{-1} for N_1-methyl-Cyt, ~ 450 cm^{-1} for N_1-ethyl-Cyt and ~ 550 cm^{-1} for N_1-isopropyl-Cyt, marked by arrows in Fig. 1.

Since Cyt and its N_1-alkyl derivatives exhibit different breaking-off energies, we measured their S_1 lifetimes at the respective 0_0^0 or lowest measurable vibronic excitation by the ps pump/ionization delay technique, which are shown in Fig. 2. The 0_0^0 lifetime of cytosine is $\tau \sim 730$ ps (Fig. 2a), and the N_1-methyl- and N_1-ethylcytosine derivatives (Fig. 2b,c) also exhibit long decay times of $\tau = 600$ ps and $\tau = 930$ ps, respectively. Branching the alkyl side-chain in N_1-isopropyl-Cyt decreases the lifetime to $\tau = 100$ ps, see Fig. 2(d). The red lines are the best fits to the kinetic model described below, see also the Supporting Information (SI).

The previous lifetime estimates of $\tau = 30-45$ ps for the Cyt 0_0^0 and 0_0^0+92 cm^{-1} vibronic bands were based on the assumption that Lorentzian (lifetime) broadening dominates the rotational band contours.[32] The 15x longer lifetime measured here implies that the band contours are broadened by additional mechanisms. Among these could be the large-amplitude inversion motion of the amino group of Cyt in the S_0 and S_1 states, or J, K-dependent Coriolis couplings that were not considered in ref. 32.

We fit the ps transients to a kinetic model in which the optically excited vibronic level S_1, v decays nonradiatively to S_0 by internal conversion (IC) with the rate $k_{IC,v}^{S_1}$, to the triplet state (here assumed to be T_1) with the intersystem crossing (ISC) rate constant $k_{ISC,v}^{S_1}$, and radiatively with the radiative rate constant $k_{rad}^{S_1}$. We fit the decay of the S_1 ($^1\pi\pi^*$) population to the differential

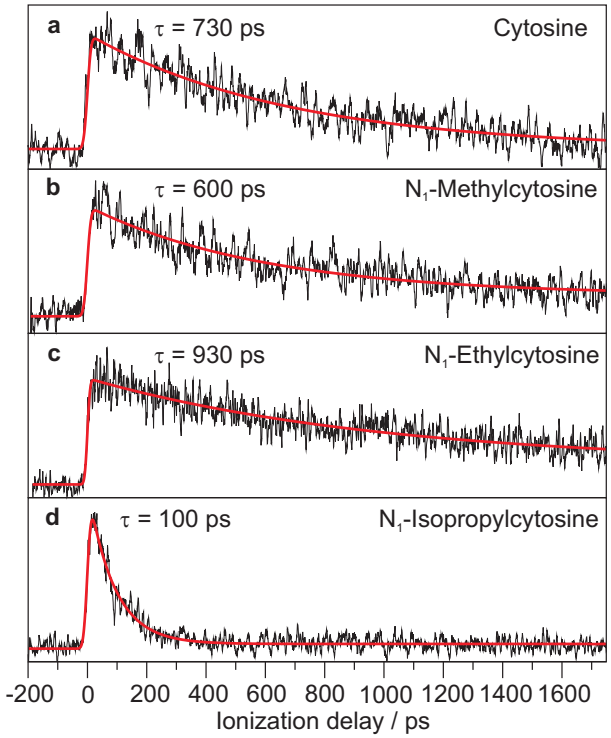

Figure 2: Picosecond time-resolved pump/delayed ionization transients of (a) Cyt (at its 0_0^0 band), (b) N_1-methyl-Cyt ($0_0^0 + 66$ cm^{-1} band), (c) N_1-ethyl-Cyt (0_0^0 band) (d) N_1-isopropyl-Cyt($0_0^0 + 44$ cm^{-1} band), ionization at 213 nm. The lifetimes τ are defined in the text.

equation

$$\frac{d[S_1]}{dt} = -(k_{IC,v}^{S_1} + k_{ISC,v}^{S_1} + k_{rad}^{S_1}) \cdot [S_1] \tag{1}$$

where $k_{IC,v}^{S_1}$ and $k_{ISC,v}^{S_1}$ depend on the vibrational level v pumped by the laser, and k_{rad} is assumed to be independent of v. The radiative lifetime $\tau_{rad} = (k_{rad})^{-1}$ of cytosine calculated at the SCS-CC2/aug-cc-pVDZ level is 18 ns, corresponding to $k_{rad} = 5.5 \cdot 10^7$ s^{-1}; those of the N_1-substituted cytosines are somewhat shorter and are given in Table S1 (Supplemental Information=SI). The triplet state is populated with the rate $k_{ISC,v}^{S_1}$ and relaxes to S_0 by $T_1 \rightsquigarrow S_0$ ISC and phosphorescence with the rate constant $k_T = k_{ISC}^{T_1} + k_{phos}$ according to:

$$\frac{d[T_1]}{dt} = k_{ISC,v}^{S_1} \cdot [S_1] - k_T \cdot [T_1] \tag{2}$$

Since we ionize at 213 nm, where both the S_1 and T_1 states can be ionized,[29–32] some of the low-v

ps transients exhibit a noticeable growing-in of the T_1 population, see Figs. S1-S3 (SI). On the other hand, the $T_1 \rightsquigarrow S_0$ decay time $1/k_T$ is on the order of $200 - 400$ ns,[29–32] far beyond the time scale of our ps pump/ionization experiments. The lifetimes τ marked in Fig. 2 for increasing excess energy E_{exc} correspond to the S_1 state decay times $\tau = (k^{S_1}_{IC,v} + k^{S_1}_{ISC,v} + k^{S_1}_{rad})^{-1}$, which are dominated by $k^{S_1}_{IC,v} + k^{S_1}_{ISC,v}$.

Fig. 3 plots the S_1 state lifetimes of Cyt and its N_1-alkyl derivatives vs. the vibrational excess energy E_{exc}; for detailed lifetimes and error estimates see Table S1 (SI). The ps pump/probe transients to which the lifetimes were fitted are shown in Figures S1-S3 (SI). Starting from the S_1 0^0_0

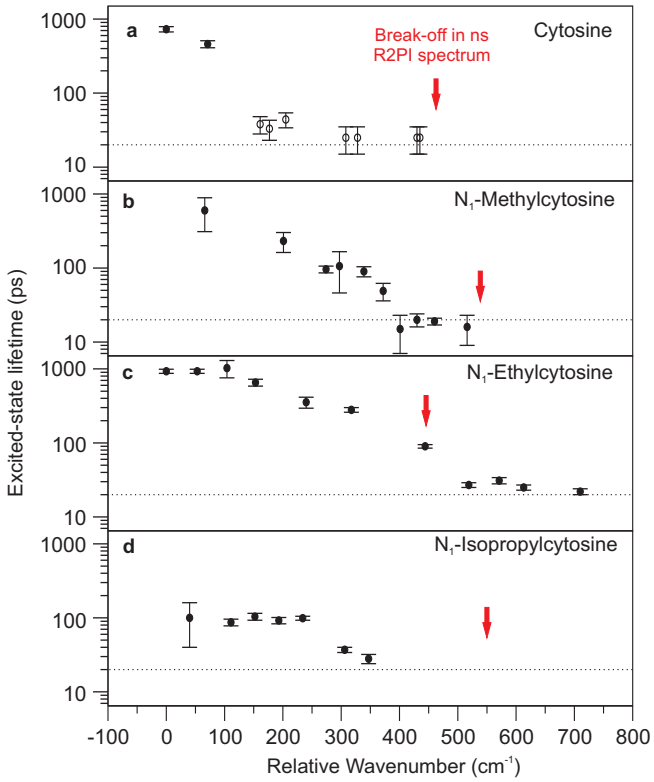

Figure 3: Dependence of the S_1 state vibronic level lifetimes of (a) Cyt, (b) N_1-methyl-Cyt, (c) N_1-ethyl-Cyt and (d) N_1-isopropyl-Cyt on the S_1 state vibrational excess energy E_{exc}. Note the logarithmic scale. In (a), the vibronic level lifetimes of Cyt marked by ∘ are from line-broadening measurements.[32] All other lifetimes (marked by •) are measured by ps pump/delayed ionization.

(or lowest measurable) vibronic band the experimental lifetimes generally decrease with increasing excess vibrational energy E_{exc}, reaching $\tau < 30$ ps at $E_{exc} = 350 - 550$ cm^{-1}. For 1-ethyl-Cyt, however, the lifetimes of the first and second out-of-plane vibronic excitations increase relative to

the $v' = 0$ level. Fig. 3 also shows that the ns laser R2PI spectra in Fig. 1 break off at approximately the vibrational excess energy E_{exc} at which the lifetime decreases below 20 ps, as marked by a dotted line.

The ps pump/ionization transients shown in Fig. 2 and in Figs. S1-S3 exhibit minor contributions from the long-lived T_1 population,[35] allowing to estimate ISC rate constants $k_{ISC,v}^{S_1}$. However, these need to be corrected for the relative ionization cross sections of the S_1 and T_1 states, $\sigma_{ion}(S_1)/\sigma_{ion}(T_1)$.[35] In ref. 35 we have shown for Cyt that they differ by a factor of ~ 3, but for the N_1-substituted cytosines they have not yet been determined. In Table S1 we therefore indicate only a few $k_{ISC,v}^{S_1}$ values, which were calculated for $\sigma_{ion}(S_1)/\sigma_{ion}(T_1) = 1 - 2$ and which should be considered as rough estimates; a fuller analysis will be given elsewhere. For the lowest vibronic levels, $k_{ISC,v}$ is in the range $0.3 - 4 \cdot 10^8$ s^{-1} and $k_{IC,v}^{S_1}$ is in the range $1 - 10 \cdot 10^9$ s^{-1}.

The ps pump/ionization delay measurements show that the near-minimum region of the S_1 $^1\pi\pi^*$ state of these cytosines must be deep enough and well enough isolated from the S_0 state (or from the perturbing S_2 state, see below) to prevent ultrafast $S_1 \rightsquigarrow S_0$ internal conversion that occurs at higher vibrational excess energies $E_{exc} = 1500 - 4000$ cm^{-1} above the $S_1, v = 0$ level.[33,34] As shown in Fig. 1, the ns laser $S_0 \rightarrow S_1$ two-color R2PI spectra break off between $300 - 550$ cm^{-1} above the electronic origins. The lifetime measurements in Fig. 3 show that the spectral breaking-off correlates well with the excess energy at which the vibronic lifetimes decrease to $\tau = 20$ ps.

We interpret the short lifetime breaking-off in terms of the heights of barriers on the S_1 state surface that "protect" the S_1 state minimum from the lowest C_5-twist conical intersection, as has been predicted by several computational studies.[12,16–23,25,28] For Cyt, the purely electronic barriers have been calculated to lie $850 - 1600$ cm^{-1} ($0.1 - 0.2$ eV) above the $^1\pi\pi^*$ state minimum.[12,21,22,28,37] However, the relevant barrier for comparison to experiment is not the electronic barrier, but the *vibrationally adiabatic* barrier, which includes the vibrational zero-point energies of the activated complex (at the barrier) and that of the S_1 minimum. The vibrationally adiabatic barrier could be significantly higher or lower than the electronic barrier and has not yet been calculated.

Increasing the N_1-alkyl group length first increases the $v' = 0$ lifetime, but the chain branching

with the isopropyl substituent decreases the lifetime by 7 times, relative to Cyt. The additional methyl group of N_1-isopropyl-Cyt strongly increases the density of internal-rotation states[38] in both the S_0 and S_1 states, which is expected to enhance the $S_1 \rightsquigarrow S_0$ internal conversion rate. However, if the density-of-states increase were the main factor determining k_{IC}, we expect to observe a significant lifetime decrease between cytosine and N_1-methyl-Cyt, in contrast to what is observed. Malone et al. observed that 5-methylation of cytosine and cytidine actually *increases* the S_1 lifetime in aqueous solution by a factor of 7,[7] and interpreted this in terms of the intermediacy of the close-lying $^1n_O\pi*$ excited state.[7,16] Excited-state lifetime changes of uracil, 5-fluorouracil and cyclohexyluracil in solution have also been interpreted in terms of differential solvent effects acting on the close-lying $^1n_O\pi^*$ and $^1\pi\pi^*$ excited states.[39,40]

We investigated the influence of N_1-alkylation on the excited states of Cyt using the SCS-CC2 method (see below for computational details). The calculated $^1\pi\pi^*$ and $^1n_O\pi^*$ energies are shown in Fig. 4. The $^1n_O\pi^*$ states of Cyt and N_1-methyl-Cyt are $2700 - 3100$ cm^{-1} vertically above the $^1\pi\pi^*$ state; the gap decreases only slightly for N_1-ethyl-Cyt. However, N_1-isopropyl substitution stabilizes the $^1n_O\pi^*$ state, rendering it almost degenerate with the $^1\pi\pi^*$ state. This near-degeneracy of $^1n_O\pi^*$ and $^1\pi\pi^*$ states is in qualitative agreement with the decrease of lifetimes between N_1-ethyl-Cyt and N_1-isopropyl-Cyt, see Figs. 2 and 3. Clearly, the $^1n_O\pi^*$ state energies follow a trend that depends more on the structure of the N_1-alkyl chain than on its length. The $^1n_O\pi^*$ state is optically "dark", so $^1n_O\pi^*$/$^1\pi\pi^*$ state mixing by itself should *increase* the excited-state lifetime if only radiative decay is considered. However, the $^1n_O\pi^*$/$^1\pi\pi^*$ state mixing may affect the height of the barrier between the $^1\pi\pi^*$ minimum and the conical intersection, thereby increase the S_1/S_0 coupling and the internal conversion rate, as schematically indicated in Fig. 4. This involvement of the lowest $^1n\pi^*$ state is in agreement with the current consensus in solution-phase photophysical studies of pyrimidine nucleobases - and cytosine in particular - that the relaxation involves branching between decay to S_0 and population of longer-lived $^1n\pi^*$ and $^3\pi\pi^*$ states.[2,7,10,16,39–41]

Summarizing, the nonradiative decay of the $S_1(^1\pi\pi^*)$ states of keto-amino Cyt and its N_1-derivatives are not *inevitably* ultrafast. The $S_1(^1\pi\pi^*)$ ($v' = 0$) lifetimes of Cyt and N_1-methyl-Cyt

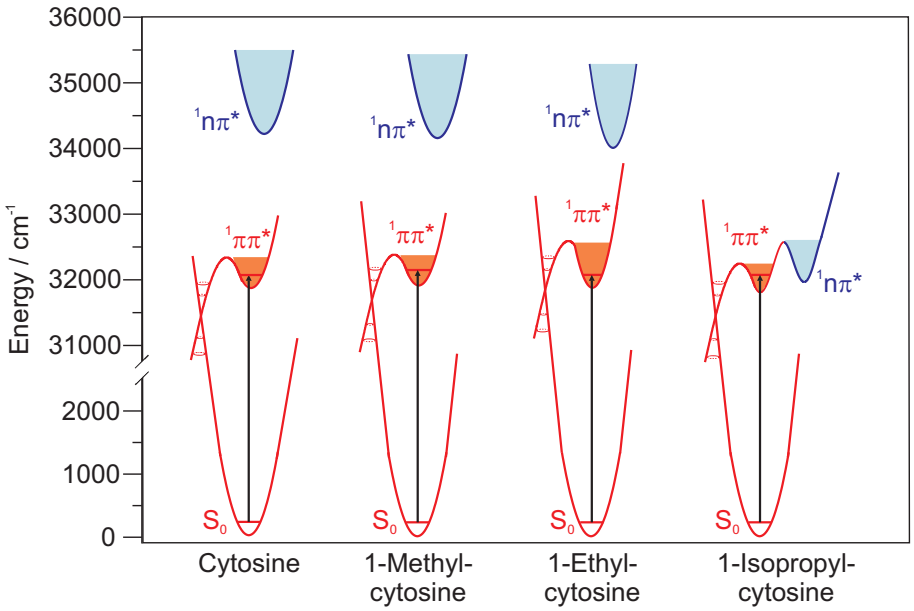

Figure 4: Schematic potential energy surfaces of the ground and lowest singlet excited states of Cyt, N_1-methyl-, N_1-ethyl- and N_1-isopropyl-Cyt. Adiabatic energies calculated at the SCS-CC2 level, barriers between the $^1\pi\pi^*$ minima and the C5-twist CI estimated from the R2PI spectral break-offs. Two excited-state rotamers exist for N_1-isopropylcytosine; the $^1\pi\pi^*$ and $^1n_O\pi^*$ minima are those of the lowest-energy conformer.

are $\tau = 600 - 730$ ps, increasing to $\tau = 1030$ ps for N_1-ethyl-Cyt at its low-lying $0_0^0 + 104$ cm^{-1} vibronic level. For Cyt, these direct ps lifetime measurements yield lifetimes that are 15 times longer than the previous indirect measurements via Lorentzian line-broadening.[32] The ISC rate constant for $S_1; v = 0$ Cyt is $\sim 10^8$ s^{-1}, see Table S1, in rough agreement with that previously determined for Cyt by nanosecond pump/ionization.[35] It will be necessary to correct the k_{IC} and k_{ISC} constants for the relative S_1 and T_1 ionization cross sections. The nonradiative decay of keto-amino cytosine and its N_1-derivatives depends sensitively on the amount of vibrational excess energy placed into the "bright" S_1 state and approaches $\tau = 20$ ps at vibrational excess energies $E_{exc} = 300 - 550$ cm^{-1}. These lifetimes extrapolate smoothly to the $\tau = 0.5 - 1.5$ ps lifetimes measured for keto-amino Cyt by fs pump/probe ionization at even higher excess energy $E_{exc} = 1500 - 4000$ cm^{-1},[33,34] and do not contradict the dynamics at higher energy. The nonradiative decay rate exhibits a marked dependence on the structure of the N_1-alkyl chain. SCS-CC2 calculations suggest that this might arise from the coupling of the very close-lying $S_2(^1n_O\pi^*)$ with the $S_1(^1\pi\pi^*)$

state.

More experiments and calculations are needed to decide whether the lifetime changes are mainly due to electronic effects, such as $^1n_O\pi^*/^1\pi\pi^*$ state mixing, or to vibrational effects such as vibrational/internal-rotation level densities. Extension of these measurements to the cytosine hydroxy-enol tautomers – which cannot be formed by the N_1 derivatives – and to complexes (cytosine base-pairs, microhydrate clusters) should also be possible.

Experimental and Computational Methods

The cytosine (or N_1-alkyl derivative) is placed in a 20 Hz internally gold-plated pulsed supersonic jet nozzle that is heated to $200 - 230^\circ$ C, corresponding to vapor pressures of $0.2 - 1$ mbar. The vapor is entrained in Ne carrier gas at $1.2 - 1.8$ bar backing pressure and expanded into the source chamber. The nanosecond resonant two-photon ionization setup has been described in Refs. 29,30. The picosecond R2PI spectroscopic and pump/ionization delay measurements are performed with an EKSPLA PL2441 20 Hz Nd:YAG laser system producing $\sim$ 25 ps laser pulses. The 355 nm (14 mJ) output pumps an EKSPLA PG401 tunable UV optical parametric oscillator/amplifier (OPO/OPA) (60μJ/pulse, 20 ps pulse length, ~ 10 cm^{-1} spectral width). The Cyt (derivatives) are $S_0 \rightarrow S_1$ excited by the UV OPO/OPA and ionized by a 20 ps pulse at 213 nm (fifth harmonic of the ps Nd:YAG pump laser). The pump and ionization beams are collimated to 3 mm beam diameter by $f = 1000$ mm UV lenses and crossed with the molecular beam inside the TOF-MS ion source. For the pump/ionization delay measurements the 213 nm ionization pulse is sent over a $0 - 400$ mm long translation stage, resulting in a $0 - 2.2$ ns time delay, details are given in ref.[42]

The S_0, S_1 and S_2 state calculations were performed with the spin-component scaled coupled-cluster method with approximate treatment of doubles (SCS-CC2) and the aug-cc-pVDZ basis set; only valence electrons were correlated. The standard scaling factors $1/3$ for the same-spin and $6/5$ for the opposite-spin components enhances the accuracy of transition energies for both $\pi\pi^*$ and $n\pi^*$ states. Previous 2C-R2PI experiments have shown that the S_1 state of keto-amino Cyt is $^1\pi\pi^*$ with a distinctly non-planar geometry.[32,35] In contrast to regular CC2 and to time-dependent density functional theory (TD-DFT) with the B3LYP functional, which predict the $^1n_O\pi^*$ state with a near-planar minimum geometry as the S_1 state at its minimum, SCS-CC2 predicts the $^1\pi\pi^*$ state as S_1, with a distinctly non-planar equilibrium structure, in agreement

with experiment.[35] The S_0 and S_1 state minimum energies were fully optimized, as well as the S_2 minima of N_1-ethyl-Cyt and N_1-isopropyl-Cyt. For the latter molecules, the $^1n_O\pi^*$ energy is the minimum along the internal-rotation path of the alkyl side chain. The $S_2(^1n_O\pi^*)$ states of Cyt and N_1-methyl-Cyt could not be optimized, the energies shown in Fig. 4 are calculated vertically above the optimized S_1 structure. All calculations were performed with TURBOMOLE 6.4.[43,44]

Acknowledgements: Financial support by the Schweiz. Nationalfonds (project nos. 200020-121993 and 200020-152816) is gratefully acknowledged.

Supporting Information Available: Details of the kinetics and fitting procedure, Table S1 with S_1 state lifetimes τ, Figures S1-S3 with ps pump/ionization transients, Tables S2 and S3 with SCS-CC2 optimized S_0, S_1 and S_2 state Cartesian geometries, Table S4 with the corresponding calculated energies. This information is available free of charge via the Internet at http://pubs.acs.org.

References

(1) Crespo-Hernández, C. E.; Cohen, B.; Hare, P. M.; Kohler, B. Ultrafast Excited-State Dynamics in Nucleic Acids. *Chem. Rev.* **2004**, *104*, 1977–2019.

(2) Middleton, C. T.; de La Harpe, K.; Su, C.; Law, Y. K.; Crespo-Hernandez, C. E.; Kohler, B. DNA Excited-State Dynamics: From Single Bases to the Double Helix. *Annu. Rev. Phys. Chem.* **2009**, *60*, 217.

(3) Schreier, W. J.; Gilch, P.; Zinth, W. Early Events of DNA Photodamage. *Annu. Rev. Phys. Chem.* **2015**, *66*, 497–519.

(4) Pecourt, J. M.; Peon, J.; Kohler, B. Ultrafast Internal Conversion of Electronically Excited RNA and DNA Nucleosides in Water. *J. Am. Chem. Soc.* **2000**, *122*, 9348–9349.

(5) Peon, J.; Zewail, A. H. DNA/RNA Nucleotides and Nucleosides: Direct Measurement of

Excited-State Lifetimes by Femtosecond Fluorescence Up-conversion. *Chem. Phys. Lett.* **2001**, *348*, 255–262.

(6) Onidas, D.; Markovitsi, D.; Marguet, S.; Sharonov, A.; Gustavsson, T. Fluorescence properties of DNA nucleosides and nucleotides: A refined steady-state and femtosecond investigation. *J. Phys. Chem. B* **2002**, *106*, 11367.

(7) Malone, R. J.; Miller, A. M.; Kohler, B. Singlet Excited-state Lifetimes of Cytosine Derivatives Measured by Femtosecond Transient Absorption. *Photochem. Photobiol.* **2003**, *77*, 158–164.

(8) Sharonov, A.; Gustavsson, T.; Carré, V.; Renault, E.; Markovitsi, D. Cytosine Excited State Dynamics Studied by Femtosecond Spectroscopy. *Chem. Phys. Lett.* **2003**, *380*, 173–180.

(9) Blancafort, L.; Cohen, B.; Hare, P. M.; Kohler, B.; Robb, M. A. Singlet Excited-State Dynamics of 5-Fluorocytosine and Cytosine: An Experimental and Computational Study. *J. Phys. Chem. A* **2005**, *109*, 4431–4436.

(10) Ma, C.; Cheng, C.-W.; Chan, C.-L.; Chan, R.-T.; Kwok, W. M. Remarkable Effects of Solvent and Substitution on the Photo-Dynamics of Cytosine: a Femtosecond Broadband Time-resolved Fluorescence and Transient Absorption Study. *Phys. Chem. Chem. Phys.* **2015**, *17*, 19045–19057.

(11) Pecourt, J. M.; Peon, J.; Kohler, B. DNA Excited-state Dynamics: Ultrafast Internal Conversion and Vibrational Cooling in a Series of Nucleosides. *J. Am. Chem. Soc.* **2001**, *123*, 10370–10378.

(12) Merchán, M.; Serrano-Andrés, L. Ultrafast Internal Conversion of Excited Cytosine via the Lowest $\pi\pi^*$ Electronic Singlet States. *J. Am. Chem. Soc.* **2003**, *125*, 8108–8109.

(13) Brauer, B.; Gerber, R. B.; Kabelač, M.; Hobza, P.; Bakker, J. M.; Riziq, A. G. A.; de Vries, M. S. Vibrational Spectroscopy of the Guanine-Cytosine Base Pair: Experiment,

Harmonic and Anharmonic Calculations and the Nature of the Anharmonic Couplings. *J. Phys. Chem. A* **2005**, *109*, 6974–6984.

(14) Serrano-Andrés, L.; Merchán, M. Are the Five Natural DNA/RNA Base Monomers a Good Choice from Natural Selection? *J. Photochem. Photobiol. C* **2009**, *10*, 21–32.

(15) Gustavsson, T.; Sharonov, A.; Markovitsi, D. Thymine, Thymidine and Thymidine 5 '-Monophosphate Studied by Femtosecond Fluorescence Upconversion Spectroscopy. *Chem. Phys. Lett.* **2002**, *351*, 195–200.

(16) Ismail, N.; Blancafort, L.; Olivucci, M.; Kohler, B.; Robb, M. Ultrafast Decay of Electronically Excited Singlet Cytosine via a $\pi\pi^*$ to $n_O\pi^*$ State Switch. *J. Am. Chem. Soc.* **2002**, *124*, 6818–6819.

(17) Blancafort, L.; Robb, M. A. Key Role of a Threefold State Crossing in the Ultrafast Decay of Electronically Excited Cytosine. *J. Phys. Chem. A* **2004**, *108*, 10609–10614.

(18) Tomic, K.; Tatchen, J.; Marian, C. M. Quantum Chemical Investigation of the Electronic Spectra of the Keto, Enol and Keto-Imine Tautomers of Cytosine. *J. Phys. Chem. A* **2005**, *109*, 8410–8418.

(19) Zgierski, M. Z.; Patchkovskii, S.; Fujiwara, T.; Lim, E. C. On the Origin of the Ultrafast Internal Conversion of Electronically Excited Pyrimidine Bases. *J. Phys. Chem. A* **2005**, *109*, 9384–9387.

(20) Merchán, M.; Gonzalez-Luque, R.; Climent, T.; Serrano-Andrés, L.; Rodríguez, E.; Reguero, M.; Peláez, D. Unified Model for the Ultrafast Decay of Pyrimidine Nucleobases. *J. Phys. Chem. B* **2006**, *110*, 26471–26476.

(21) Blancafort, L. Energetics of Cytosine Singlet Excited-State Decay Paths - A Difficult Case for CASSCF and CASPT2. *J. Photochem. Photobiol.* **2007**, *83*, 603–610.

(22) Kistler, K. A.; Matsika, S. Radiationless Decay Mechanism of Cytosine: An Ab Initio Study with Comparisons to the Fluorescent Analogue 5-Methyl-2-pyrimidinone. *J. Phys. Chem. A* **2007**, *111*, 2650–2661.

(23) Hudock, H. R.; Martínez, T. J. Excited-State Dynamics of Cytosine Reveal Multiple Intrinsic Subpicosecond Pathways. *Chem. Phys. Chem.* **2008**, *9*, 2486–2490.

(24) González-Vazquez, J.; González, L. A Time-Dependent Picture of the Ultrafast Deactivation of keto-Cytosine Including Three-State Conical Intersections. *ChemPhysChem* **2010**, *11*, 3617–3624.

(25) Barbatti, M.; Aquino, A. J. A.; Szymczak, J. J.; Nachtigallova, D.; Lischka, H. Photodynamical Simulations of Cytosine: Characterization of the Ultrafast Bi-Exponential UV Deactivation. *Phys. Chem. Chem. Phys.* **2011**, *13*, 6145–6155.

(26) Richter, M.; Marquetand, P.; Gonzalez-Vazquez, J.; Sola, I.; Gonzalez, L. Femtosecond Intersystem Crossing in the DNA Nucleobase Cytosine. *J. Phys. Chem. Letters* **2012**, *3*, 3090–3095.

(27) Mai, S.; Marquetand, P.; Richter, M.; Gonzalez-Velasquez, J.; Gonzalez, L. Singlet and Triplet Excited-State Dynamics Study of the Keto and Enol Tautomers of Cytosine. *ChemPhysChem* **2013**, *14*, 2920–2931.

(28) Nakayama, A.; Yamazaki, S.; Taketsugu, T. Quantum Chemical Investigations on the Nonradiative Deactivation Pathways of Cytosine Derivatives. *J. Phys. Chem. A* **2014**, *118*, 9429–9437.

(29) Nir, E.; Müller, M.; Grace, L. I.; de Vries, M. S. REMPI Spectroscopy of Cytosine. *Chem. Phys. Lett.* **2002**, *355*, 59–64.

(30) Nir, E.; Hünig, I.; Kleinermanns, K.; de Vries, M. S. The Nucleobase Cytosine and the Cy-

tosine Dimer Investigated by Double-Resonance Laser Spectroscopy and Ab Initio Calculations. *Phys. Chem. Chem. Phys.* **2003**, *5*, 4780–4785.

(31) Lobsiger, S.; Leutwyler, S. The Adiabatic Ionization Energy and Triplet T_1 Energy of Jet-Cooled Keto-Amino Cytosine. *J. Phys. Chem. Lett.* **2012**, *3*, 3576–3580.

(32) Lobsiger, S.; Trachsel, M. A.; Frey, H. M.; Leutwyler, S. Excited-State Dynamics of Cytosine: The Decay of the Keto-Amino Tautomer is Not Ultrafast. *J. Phys. Chem. B* **2013**, *117*, 6106–6115.

(33) Kosma, K.; Schröter, C.; Samoylova, E.; Hertel, I. V.; Schultz, T. Excited-State Dynamics of Cytosine Tautomers. *J. Am. Chem. Soc* **2009**, *131*, 16939–16943.

(34) Ho, J. W.; Yen, H.-C.; Chou, W.-K.; Weng, C.-N.; Cheng, L.-H.; Shi, H.-Q.; Lai, S.-H.; Cheng, P.-Y. Disentangling Intrinsic Ultrafast Excited-State Dynamics of Cytosine Tautomers. *J. Phys. Chem. A* **2011**, *115*, 8406–8418.

(35) Lobsiger, S.; Etinski, M.; Blaser, S.; Frey, H.-M.; Marian, C.; Leutwyler, S. Intersystem Crossing Rates of S_1 State Keto-Amino Cytosine at Low Excess Energy. *J. Chem. Phys.* **2015**, *143*, 234301–1–12.

(36) Trachsel, M. A.; Lobsiger, S.; Leutwyler, S. Out-of-Plane Low-Frequency Vibrations and Nonradiative Decay in the $^1\pi\pi^*$ State of Jet-Cooled 5-Methylcytosine. *J. Phys. Chem. B* **2012**, *116*, 11081–11091.

(37) Blancafort, L.; Bearpark, M. J.; Robb, M. A. In *Computational modeling of cytosine photophysics and photochemistry: from the gas phase to DNA, in radiation induced molecular phenomena in nucleic acids*; Shukla, M. K., Leszczynski, J., Eds.; M. K. Shukla and J. Leszczynski (eds), Springer, Netherlands, pp 473–492, 2008.

(38) Alvarez-Valtierra, L.; Tan, X.-Q.; Pratt, D. W. On the Role of Methyl Torsional Modes in the

Intersystem Crossing Dynamics of Isolated Molecules. *J. Phys. Chem. A* **2007**, *111*, 12802–12809.

(39) Hare, P. M.; Crespo-Hernandez, C. E.; Cohen, B.; Kohler, B. Internal Conversion to the Electronic Ground State Occurs via two Distinct Pathways for Pyrimidine Bases in Aqueous Solution. *Proc. Natl. Acad. Sci. USA* **2007**, *104*, 435–440.

(40) Santoro, F.; Barone, V.; Gustavsson, T.; Improta, R. Solvent Effect on the Singlet Excited-state Lifetimes of Nucleic Acid Bases: A Computational Study of 5-Fluorouracil and Uracil in Acetonitrile and Water. *J. Am. Chem. Soc.* **2006**, *128*, 16312–16322.

(41) Hare, P. M.; Crespo-Hernandez, C. E.; Cohen, B.; Kohler, B. Solvent-Dependent Photophysics of 1-Cyclohexyluracil: Ultrafast Branching in the Initial Bright State. *J. Phys. Chem. B* **2006**, *110*, 18641–18650.

(42) Blaser, S.; Frey, H.-M.; Heid, C. G.; Leutwyler, S. Gas-Phase Lifetimes of Nucleobase Analogues by Picosecond Pump-ionization and Streak Techniques. *Chimia* **2014**, *86*, 260–283.

(43) TURBOMOLE *V6.4 2013*; A Development of Universität Karlsruhe (TH) and Forschungszentrum Karlsruhe GmbH, 1989-2007, TURBOMOLE GmbH; available from `http://www.turbomole.com`. (accessed May 19, 2015).

(44) The thresholds for SCF and one-electron density convergence were set to 10^{-9} a.u. and 10^{-8} a.u., respectively. The convergence thresholds for all structure optimizations were set to 10^{-8} a.u. for the energy change, $6 \cdot 10^{-6}$ a.u. for the maximum displacement element, 10^{-6} a.u. for the maximum gradient element, $4 \cdot 10^{-6}$ a.u. for the RMS displacement and 10^{-6} a.u. for the RMS gradient.